horticulturae

MDPI

Article

Water Deficit Severity during the Preceding Year Determines Plant Tolerance to Subsequent Year Drought Stress Challenges: A Case Study in Damask Rose

Fatemeh Aalam [1], Abdolhossein Rezaei Nejad [1,*], Sadegh Mousavi-Fard [2], Mohammadreza Raji [1], Nikolaos Nikoloudakis [3], Eleni Goumenaki [4] and Dimitrios Fanourakis [4]

[1] Department of Horticultural Sciences, Faculty of Agriculture, Lorestan University, Khorramabad P.O. Box 465, Iran; fa.aalam29@gmail.com (F.A.); raji.m@lu.ac.ir (M.R.)
[2] Department of Horticultural Science, Faculty of Agriculture, Shahrekord University, Shahrekord P.O. Box 115, Iran; sadeghmosavifard@gmail.com
[3] Department of Agricultural Sciences, Biotechnology and Food Science, Cyprus University of Technology, Limassol CY-3603, Cyprus; n.nikoloudakis@cut.ac.cy
[4] Laboratory of Quality and Safety of Agricultural Products, Landscape and Environment, Department of Agriculture, School of Agricultural Sciences, Hellenic Mediterranean University, Estavromenos, 71004 Heraklion, Greece; egoumen@hmu.gr (E.G.); dimitrios.fanourakis82@gmail.com (D.F.)
* Correspondence: rezaeinejad.h@lu.ac.ir

Abstract: Damask rose is an important essential oil crop. In the present study, plants were subjected to three different water deficit levels (70, 40, and 10% available water content) for two periods (June–October). Plant phenology, growth, essential oil yield, gas exchange features, membrane stability and major antioxidant defense elements were monitored across two years. Soil water deficit was related to quicker completion of the growth cycle (up to 7.4 d), and smaller plants (up to 49.7%). Under these conditions, biomass accumulation was jointly constrained by decreased leaf area, chlorophyll content, CO_2 intake, and photosynthetic efficiency (up to 82.8, 56.9, 27.3 and 68.2%, respectively). The decrease in CO_2 intake was driven by a reduction in stomatal conductance (up to 41.2%), while the decrease in leaf area was mediated by reductions in both number of leaves, and individual leaf area (up to 54.3, and 64.0%, respectively). Although the reactive oxygen species scavenging system was activated (i.e., proline accumulation, and enhanced activity of three antioxidant enzymes) by water deficit, oxidative stress symptoms were still apparent. These effects were amplified, as soil water deficit became more intense. Notably, the adverse effects of water deficit were generally less pronounced when plants had been exposed to water severity during the preceding year. Therefore, exposure to water deficit elicited plant tolerance to future exposure. This phenotypic response was further dependent on the water deficit level. At more intense soil water deficit across the preceding year, plants were less vulnerable to water deficit during the subsequent one. Therefore, our results reveal a direct link between water deficit severity and plant tolerance to future water stress challenges, providing for the first time evidence for stress memory in damask rose.

Keywords: antioxidant defense; biomass accumulation; carbon assimilation; cellular damage; flowering; *Rosa damascena*; water deprivation

Citation: Aalam, F.; Rezaei Nejad, A.; Mousavi-Fard, S.; Raji, M.; Nikoloudakis, N.; Goumenaki, E.; Fanourakis, D. Water Deficit Severity during the Preceding Year Determines Plant Tolerance to Subsequent Year Drought Stress Challenges: A Case Study in Damask Rose. *Horticulturae* **2024**, *10*, 462. https://doi.org/10.3390/horticulturae10050462

Received: 19 March 2024
Revised: 24 April 2024
Accepted: 29 April 2024
Published: 1 May 2024

1. Introduction

Damask rose (*Rosa damascena* Mill.) ranks among the top in the list of high-value essential oil crops [1,2]. It is a perennial shrub, which is commercially cultivated in many countries across the world (e.g., Bulgaria, China, Egypt, France, India, Iran, Italy, Morocco, Russia, Turkey, and the USA) [3–5]. Although at present the essential oil of damask rose is mostly employed by fragrance and food industries, it has repeatedly been shown to demonstrate great potential for cosmetic and pharmaceutical applications owing to a wide range of acquired therapeutic, antimicrobial, and antioxidant properties [1,6,7]. On a global

scale, it has been estimated that the demand currently exceeds production by a factor of two, while the former is expected to rise substantially in the near future [3,5]. This demand–supply gap is further challenged by the frequently recorded declining rainfall events in semiarid and rainfed sites [8,9]. Since the occurrence of water deficit events is likely to increase in environments with low or unpredictable precipitation, elucidating the respective plant responses will likely provide guidance towards yield improvements [10].

Several morphological and physiological traits are adversely affected by water deficit, and collectively limit plant growth and productivity [11–13]. Under water deficit conditions, for example, photosynthesis is jointly constrained by decreases in stomatal conductance (CO_2 intake), leaf area (light interception), chlorophyll content (light absorption) and photosynthetic efficiency [9,14]. Under these conditions, the coordination between the generation and detoxification of reactive oxygen species (ROS) is also weaker [15]. Antioxidant defense comprises of both enzymatic [e.g., ascorbate peroxidase (APX), catalase (CAT) and peroxidase (POD)] and non-enzymatic (e.g., carotenoids) components [14,16]. ROS scavenging properties have also been ascribed to proline, which exerts a range of additional beneficial functions such as balancing osmotic pressure as well as maintaining protein and cell membrane stability [9,15]. Under increased ROS accumulation, many adverse effects are unavoidable, including lipid peroxidation and the associated electrolyte leakage [16,17].

The literature associated with water deficit effects is conventionally limited to a single crop cycle or shorter periods [8,14,18,19]. Although this approach is suitable for annual taxa, it is evidently less informative for perennial ones [12]. The few existing studies suggest that some species adjust certain morphological and physiological traits, which may change plant ability to endure next season's stress events (the so-called stress memory) [12,20–22]. This acclimation considerably diverged between species [23,24], justifying the need to investigate more taxa of interest. In addition, the relation between growth history and plant response to next-season stress events has been mostly evaluated qualitatively, namely by realizing a single water deficit level [12,24]. Therefore, a quantitative analysis between water deficit severity and plant phenotype following the next season stress event has not currently been determined.

In this context, the quantitative relationship between water deficit severity and plant phenotype was investigated across two consecutive years. Plants were subjected to three different water deficit levels for two seasons. Alongside to essential oil yield, emphasis was placed on plant phenology, photosynthetic efficiency, gas exchange features, membrane stability, and major antioxidant defense systems. The following hypotheses were addressed: (i) the acclimation level to water deficit depends on the severity of water limitation; and (ii) differences in acclimation level are associated with morphological, physiological and biochemical alterations. The present physiological approach is expected to generate valuable insights into tolerance to environments with low water availability, which in the long run may potentially manage effective and sustainable damask rose essential oil production.

2. Materials and Methods

2.1. Plant Material and Growth Conditions

The present field study was performed at the experimental farm of the Faculty of Agriculture of Lorestan University (semi-arid climate region) in Khorramabad (Iran), at 33°29′ N latitude, 48°22′ E longitude and 1125 m altitude. Soil (0−40 cm depth) was of fine texture (45.3% clay, 32.2% silt and 22.5% sand) with 0.4% organic carbon content, and 2.4 dS m^{-1} electrical conductivity. Prior to experimental year 1 (2017−2018), soil N, P, and K contents were 0.060%, 11.8 ppm, and 275 ppm, while prior to experimental year 2 (2018−2019) these were 0.058%, 12.04 ppm, and 268 ppm, respectively. Field management followed conventional local practices. Fertilizer application (118, 128, and 176 kg per hectare net amounts of N, P and K, respectively) was practiced every year at two doses (1 March, and 15 April), and was decided by considering soil analysis and nutrient requirements of damask rose. On a regular basis, weeds were manually removed. Pesticide or fungicide use was not required.

The damask rose Iranian cv. "Kashan 93" was employed, because it is water deficit -tolerant, and is commonly cultivated in Iran. To overcome the difficulty of forming adventitious roots, single-node leafy (semi-hardwood) stem cuttings were rooted in vitro (10.26 ± 1.21 roots per shoot). For experimentation, rooted cuttings were selected to be of similar leaf area (38–42 cm^2), shoot diameter (5−6 mm) and vigor. These were manually transplanted in the field on 14 November (2017). Two cuttings were initially planted per spot. Two weeks later, the most vigorous one was kept at each spot, by removing the other one. The distance between (north–south oriented) rows and plants was 1.5 and 0.75 m, respectively (thus at a density of 0.88 plants m^{-2}).

The experiment lasted for 3 successive years (2017−2020). In the first year (2017−2018; hereafter referred to as experimental year 1), the three water deficit treatments (described below) were realized from June to October of 2018 (i.e., immediately after the spring rains, and lasted until the start of autumn rains). Morphological, physiological and biochemical traits were evaluated at the end of the treatment (i.e., 1–5 d before the autumn rains of 2018), while phenology and flowering features were assessed in the spring (April–May) of the subsequent year (2019). Likewise, in the second year (2018−2019; hereafter referred to as experimental year 2), treatments were performed from June to October of 2019 (i.e., after the spring rains and until the start of autumn rains). Morphological, physiological and biochemical traits were determined at the end of the treatment (i.e., 1–5 d before autumn rains of 2019), while phenology and flowering traits were recorded in the spring (April–May) of the next year (2020).

During the abovementioned period (June–October; absence of precipitation) of experimental year 1 (2017−2018), three water deficit levels were implemented, by adjusting irrigation to 70, 40, and 10% available water content (representing full irrigation, mild water deficit, and severe water deficit, respectively). The employed available water content range was selected on the basis of both a comprehensive literature survey [8,18], and a pre-experiment. Prior to the experiment, a preliminary study, covering an extended range of irrigation levels, informed choice of the irrigation regime by which the crop was optimally grown (thus avoiding excess irrigation), as well as the one where growth is severely impeded, meanwhile minimizing the risk of mortality.

The respective water deficit level was maintained by adjusting irrigation volume based on soil water content, when the required threshold was reached. Soil water content was determined at the depth of 5–20 cm by using time domain reflectometry probes (CS630/CS635, Campbell Scientific Ltd., Leicestershire, UK). Regardless of the water deficit level, the same quantity of nutrients was supplied to all plants. In each treatment, the abovementioned water deficit levels (70, 40, and 10% available water content) were also applied during the abovementioned period (June–October) of experimental year 2 (2018–2019). The experiment thus consisted of nine treatments [3 water deficit regimes (year 1) × 3 water deficit regimes (year 2)]. The experimental plots were distributed according to a factorial arrangement following a randomized complete block design. Each plot contained four lines in sequence (Figure S1). At each plot, measurements were performed on three randomly selected plants situated at lines 2 and 3 (thus excluding the border lines 1 and 4). In each plant, three separate measurements were further obtained. The average of nine measurements [i.e., (3 plants $plot^{-1}$) × (3 measurements $plant^{-1}$)] was further treated as a single replication. For taking observations, three plots were analyzed, and in this way three replications were considered.

Available water content refers to the volume of water which can be absorbed by the plant, representing the difference between field capacity and permanent wilting point. These variables were measured by employing the retention curve method and corresponded to −0.1 kPa and −1.5 MPa matric potentials, respectively. At the permanent wilting point, although soil still includes some water, it is unavailable for plant uptake.

Determinations were performed at both organ (leaf, flower) and plant levels. For leaf-level assessments, sampled leaves had developed under direct sunlight, and were fully expanded. For flower-level evaluations, fully open flowers were selected (i.e., anthers were

visible; the so-called stage V). Non-invasive determinations were carried out 1–5 d prior to the destructive harvest. In destructive measurements, the time between sampling and the onset of the evaluation never exceeded 12 min, besides enzymatic activity assessment, where samples were immediately immersed in liquid nitrogen, and moved to a freezer at −80 °C for storage before further processing.

To avoid border effects, a border row surrounded the experimental units, which was not sampled (Figure S1). In all evaluations, three replicates were assessed. Each replicate corresponded to a different plant, which was randomly sampled within every plot (excluding the border row plants). In all destructive measurements, three separate measurements were performed in each replicate plant, and further averaged. In leaf potassium and calcium content assessment (described below) specifically, these three samples per replicate plant were pooled.

2.2. Leaf Chlorophyll Fluorescence

To evaluate plant photosynthetic performance, the ratio of variable to maximum chlorophyll fluorescence (F_v/F_m) was recorded [25,26]. Measurements were carried out by employing an analyzer fluorimeter (Pocket PEA, Hansatech Instruments, King's Lynn, Norfolk, UK). Immediately after dark adaptation (≥30 min), the maximum quantum efficiency of PSII photochemistry (F_v/F_m) was measured using a photosynthetic photon flux density of 3000 μmol m^{-2} s^{-1} as saturating flash for a duration of 1 s [27].

For assessing the in vivo adaptive responses of the photosynthetic system (especially photosystem II) to the cultivation regime, the kinetics of chlorophyll fluorescence induction were further determined. In this context, a polyphasic chlorophyll fluorescence induction curve (O–J–I–P-transient) was performed [25,26]. The computations and applied protocol are provided in Moosavi-Nezhad et al. (2021) [25].

By using attached fully expanded leaves of intact plants, the above-mentioned chlorophyll fluorescence evaluations were conducted on a clear day and 1 h following the onset of the light period (07:00–09:00 h) at the growth site (Figure S1). The sampling area was outlined with a marker. Prior to each evaluation, leaves were dark adapted (≥30 min) by using leaf clips. To minimize systematic within-leaf heterogeneity, sampling areas were selected in the middle of the lamina (1 cm distance from the main vein), by excluding leaflet periphery (i.e., ≥2 cm of the leaf base and tip) [28]. Three replicates were evaluated per treatment.

2.3. Leaf Gas Exchange

By employing a portable photosynthesis system (CI-340; CID, Inc., Camas, WA, USA), leaf gas exchange features were determined. During evaluation, environmental conditions (22 °C air temperature, 50% relative air humidity, 400 μmol mol^{-1} incoming air CO_2 concentration and 2000 μmol m^{-2} s^{-1} photosynthetic photon flux density) were held constant. In order to perform the evaluations under a uniform stomatal conductance pattern, determinations were carried out on a clear day and 2 h following the onset of the light period (08:00–10:00 h) [15]. Prior to evaluation, leaves were allowed to equilibrate to leaf chamber conditions (≥15 min). Photosynthetic water use efficiency ($\frac{\text{net photosynthesis rate}}{\text{transpiration}}$) and carboxylation efficiency ($\frac{\text{net photosynthesis rate}}{\text{intracellular } CO_2 \text{ concentration}}$) were further computed. Gas exchange features were determined on the leaves on which chlorophyll fluorescence features had been earlier assessed, by using the same (marked) spot. Three replicates were evaluated per treatment.

2.4. Plant Phenology, Morphology, and Biomass Allocation

The time to flowering, number of flowers, flower diameter, number of petals, and receptacle (axis to which floral organs are attached) diameter were recorded. For evaluating flower diameter, measurements were performed in two perpendicular directions (starting from the largest diameter), and averaged. Diameter assessments were performed by using a caliper (±0.2 mm; series 500 Mitutoyo, Aurora, IL, USA).

The main stem length (from the root-to-shoot junction to the apical meristem), canopy diameter, number of leaves (longer than 0.5 cm), and leaf area (one-sided surface area) were

also measured. For canopy diameter assessment, the overhead (top-view) 2D plant silhouette was considered. A convex hull (the minimal polygon enclosing the entire plant silhouette perimeter) was fitted, and the maximum and minimum distances of point pairs intersecting the convex hull center were taken as plant length and width, respectively. By using these data, canopy area was calculated ($\pi \times$ plant length/2 $\times$ plant width/2) [13]. Stem and canopy length, as well as canopy width assessments were performed by using a folding meter (±0.1 cm). For leaf area determination, individual leaves were scanned (HP Scanjet G4010; Irvine, CA, USA), and then evaluated by using specialized software (Digimizer software; version 4.1.1.0, MedCalc Software, Ostend, Belgium) [16]. In some cases at 10% available water content, sampled leaves were moderately curled towards the midrib (see images in Jia et al., 2021 [29]). To eliminate the curvature-induced reduction in projected area, these leaves were flattened out on a white paper prior to scanning. Individual leaf area values were recorded to the nearest 1 mm^2. Plant leaf area was the sum of individual leaf areas.

Shoot, (total and individual) flower, as well as (total and individual) petal (fresh and dry) masses were further determined (±0.01 g; MXX-412; Denver Instruments, Bohemia, NY, USA). For dry weight assessment, herbal samples were transferred to a drying oven (80 °C) for 72 h. For evaluating the level of tolerance, stress tolerance index was calculated as the biomass of each treatment relative to the biomass of control ($\frac{\text{plant dry weight}}{\text{plant dry weight of control}} \times 100\%$). For assessing the ratio of plant carbon gain to water use, integral water use efficiency was computed as the ratio of plant dry mass to water use ($\frac{\text{plant dry weight}}{\text{total water consumption}}$).

2.5. Petal Essential Oil Content

The essential oil content is equally important to essential oil yield, because it directly affects the extraction cost, and in this way the financial returns of essential oil production [30,31]. By using a Clevenger apparatus, petal samples were submitted to hydro-distillation. Herbal material (500 g) was added to a 1 L flask filled with 400 mL of double-distilled water. Heating was applied for 3 h [31]. The isolated essential oils were dried over anhydrous sodium sulfate [31]. Essential oil content was expressed in percentage ($\frac{\text{essential oil weight}}{\text{sample weight}} \times 100\%$).

In the morning (07:00–09:00 h) after dew, sampling was performed (18–20 °C during harvest). To maintain turgidity, excised petal samples were immediately placed in sealable plastic bags with moistened tissue, which were placed under shade while remaining at the field site. Three replicates were assessed per sample.

2.6. Leaf Potassium and Calcium Content

The leaf potassium and calcium contents were evaluated. Leaves were cleaned with double distilled water, and placed in a drying oven (80 °C) for 72 h. They were then ground into fine powder, and filtered through a 30-mesh screen [32]. The filtered herbal material (1 g) was dry-ashed at 515 °C for 6 h. The obtained ash was dissolved in 6.0 N HCl (5 mL), and filled up to 50 mL by using double distilled water [32]. Potassium and calcium contents were assessed by using a flame photometer (Jenway PFP7, Keison, Chelmsford, Essex, UK) and atomic absorption spectrometry, respectively. These were expressed on a dry weight basis. In both elements, quantitative assessment was performed by using the respective standard curve. Three replicates were evaluated per treatment. For each replicate, three samples had been pooled.

2.7. Leaf Chlorophyll and Carotenoid Content

Leaf chlorophyll content is critical for photosynthesis, while carotenoids are essential non-enzymatic antioxidants [16]. Leaf material (0.1 g) was homogenized with 100% acetone (10 mL). The homogenate was centrifuged (14,000× g for 20 min), and the supernatant was used for the assay. As chlorophyll is light-sensitive, extraction was carried out in darkness. The obtained solution was analyzed by using a spectrophotometer (Mapada UV-1800; Shanghai Mapada Instruments Co., Ltd., Shanghai, China). Leaf chlorophyll and

carotenoid contents were calculated as described by Lichtenthaler and Wellburn (1983) [33]. Three replicates were evaluated per treatment.

2.8. Leaf Water Status

Plant water status was evaluated by recording leaf relative water content (RWC; also referred to as relative turgidity). Sampling was conducted 2 h following the onset of the light period (08:00–08:30 h). Immediately after excision, fresh weight was recorded (±0.0001 g; Mettler AE 200, Giessen, Germany). Leaves were then positioned on double distilled water in a 9 cm Petri dish, sealed with a lid. After 24 h incubation in darkness, the turgid (saturated) weight was determined. Eventually, dry weight was measured after 72 h at 80 °C. Based on these data, RWC was computed ($\frac{\text{fresh weight} - \text{dry weight}}{\text{saturated fresh weight} - \text{dry weight}} \times 100\%$) [34,35]. Three replicates were evaluated per treatment.

2.9. Leaf Electrolyte Leakage

The relative ion content in the apoplastic space (including cell membrane outer space, cell wall, intercellular spaces and apoplastic fluid), conventionally considered an indicator of membrane stability, was examined by determining electrolyte leakage [15]. Excised leaf discs (2 cm^2) were cleaned three times with double-distilled water (3 min each) to take away surface-adhered electrolytes. They were then positioned on double distilled water (10 mL), and exposed to shaking at room temperature (25 °C) for 24 h. The electrolyte leakage in the resulting solution was subsequently recorded by using a conductimeter (Crison 522, Crison Instruments, S.A., Barcelona, Spain). Eventually, samples were autoclaved at 120 °C for 20 min. Total conductivity was then determined after returning to room temperature (25 °C). Three discs were assessed per replicate leaf. Three replicates were evaluated per treatment.

2.10. Leaf Lipid Peroxidation

The malondialdehyde (MDA) content, conventionally employed as an index of lipid peroxidation level, was recorded by using the thiobarbituric acid reactive substance assay [15]. Excised leaf discs (2 cm^2) were homogenized. Then, they were immersed in 5 mL of 20% (w/v) trichloroacetic acid and 0.5% (w/v) thiobarbituric acid. Next, the suspension was subjected to centrifugation (6000× g for 15 min). The solution was then heated at 100 °C for 25 min. After reaching room temperature (25 °C), the precipitate was collected by centrifugation (6000× g for 5 min). The MDA content was computed by considering the absorbance at 532 nm, with adjustments for non-specific absorption at 450 and 600 nm, by using a spectrophotometer (Mapada UV-1800; Shanghai Mapada Instruments Co., Ltd., Shanghai, China). For the computation, an extinction coefficient (156 mmol MDA L^{-1} cm^{-1}) was employed [15]. Three discs were examined per replicate leaf. Three replicates were evaluated per treatment.

2.11. Leaf Proline Content

Proline is elemental in regulating cell osmotic balance (by reducing water potential), and in this way safeguards both enzymatic activity and macromolecules' structure [9,16]. In this context, leaf proline content was determined. Leaf samples (0.5 g) were subjected to homogenization, and then were immersed in 3% (w/v) aqueous sulphosalicylic acid (10 mL). The resulting extract was filtered (Whatman No. 2). Equal volumes of filtrate (2 mL), acid–ninhydrin (2 mL) and glacial acetic acid (2 mL) were combined. This mixture was heated to 100 °C for 1 h. The mixture was subsequently extracted with toluene (4 mL), and the (toluene-containing) chromophore was extracted from the liquid phase. After restoring room temperature (25 °C), the absorbance was measured at 520 nm by using a spectrometer (Mapada UV-1800; Shanghai. Mapada Instruments Co., Ltd., Shanghai, China). The proline concentration was determined based on a calibration curve [9,16]. Three replicates were evaluated per treatment.

2.12. Leaf Enzymatic Activity

For CAT activity assessment, leaf tissue (0.3 g) was ground with a (pre-cooled) mortar and pestle in liquid nitrogen for 5 min, homogenized with 1.5 mL of potassium phosphate buffer (containing 1 mM EDTA and 2% polyvinylpyrrolidone), and then centrifuged (14,000× *g* for 20 min) at 4 °C [15]. In the supernatant, CAT activity was determined by monitoring the decrease in absorbance at 240 nm for 2 min (10 s intervals) in a reaction mixture containing potassium phosphate buffer and hydrogen peroxide. For the computation, an extinction coefficient (39.4 M^{-1} cm^{-1}) was utilized.

For POD activity evaluation, leaf tissue (0.3 g) was ground with a (pre-cooled) mortar and pestle in liquid nitrogen for 5 min, homogenized with 1.5 mL of 50 mM potassium phosphate buffer (pH 7.0), and then centrifuged (14,000× *g* for 20 min) at 4 °C [15]. The POD activity in the supernatant was assessed by measuring the reduction in absorbance at 470 nm for 2 min (10 s intervals) in a reaction mixture consisting of potassium phosphate buffer, guaiacol, and hydrogen peroxide. For the computation, an extinction coefficient (26.6 mM^{-1} cm^{-1}) was employed.

For APX activity determination, leaf tissue (0.3 g) was ground with a (pre-cooled) mortar and pestle in liquid nitrogen for 5 min, and homogenized in the extraction solution [50 mM Na_2HPO_4/KH_2PO_4 (pH 7.0), 1 mM EDTA, 5% polyvinylpyrrolidone, and 1 mM ascorbic acid] [15]. The homogenate was then centrifuged (14,000× *g* for 20 min) at 4 °C. In the supernatant, APX activity was determined by monitoring the decrease in absorbance at 290 nm for 2 min (10 s intervals).

CAT, POD, and APX activity was expressed as μmol hydrogen peroxide reduced per min per g tissue [36]. Three replicates were evaluated per treatment.

2.13. Statistical Design and Analysis

Data analyses were carried out by using the R software (R version 4.3.1). A two-way ANOVA was applied, with the water deficit level of experimental year 1 serving as the factor A and the water deficit level of experimental year 2 as the factor B. Prior to further analysis, data was checked for normality (Shapiro–Wilk test) and homogeneity of variances (Levene's test). Estimated least significant differences (LSD) of treatment effects were calculated ($p = 0.05$).

2.14. Principal Component and Correlation Analyses

Eigenvalues were computed for each of the 27 experimental units, and the variables that contributed most to each dimension were determined (Figures S1 and S2). In order to build the principal components, the first two eigenvalues, which accounted for 76.6% of the total variance, were retained. To find relationships between the principal components and the water deficit levels, a principal component analysis (PCA) was conducted. Units were clustered (using a unique color), and variables were grouped according to how much they engaged with the main components (using gradient colors). To show the positive and negative correlations between the variables under investigation, a correlation plot was also created. Under the R-studio integrated development environment (RStudio suite, 2023.06.0 Build 421, Boston, MA, USA), the libraries 'factoextra', 'FactoMineR', 'readxl', and 'corrplot' were utilized.

3. Results

3.1. Correlation Analysis

Correlation analysis across 45 traits revealed a complex relationship between morphological and biochemical attributes, that define damask rose physiology under different water deficit levels. The majority of interactions were positively regulated and statistically significant at the 0.5 level (Figure 1). Specifically, an important trait such as the shoot dry weight was associated with the number of petals, chlorophyll content, receptacle diameter, flower dry weight and individual leaf area, while negative associations were established with MDA concentration and electrolyte leakage. In parallel, both essential oil yield and percentage were positively correlated to carboxylation efficiency, and leaf Ca

content. Interestingly, several indices such as floral water use efficiency and the relative variable fluorescence at 2 ms (V_j) remained unrelated, while the noted activation of the ROS scavenging system [i.e., proline accumulation, and enhanced activity of three antioxidant enzymes (CAT, POD, and APX)] displayed a somewhat neutral association to most of the studied traits, signifying a broader function for damask rose.

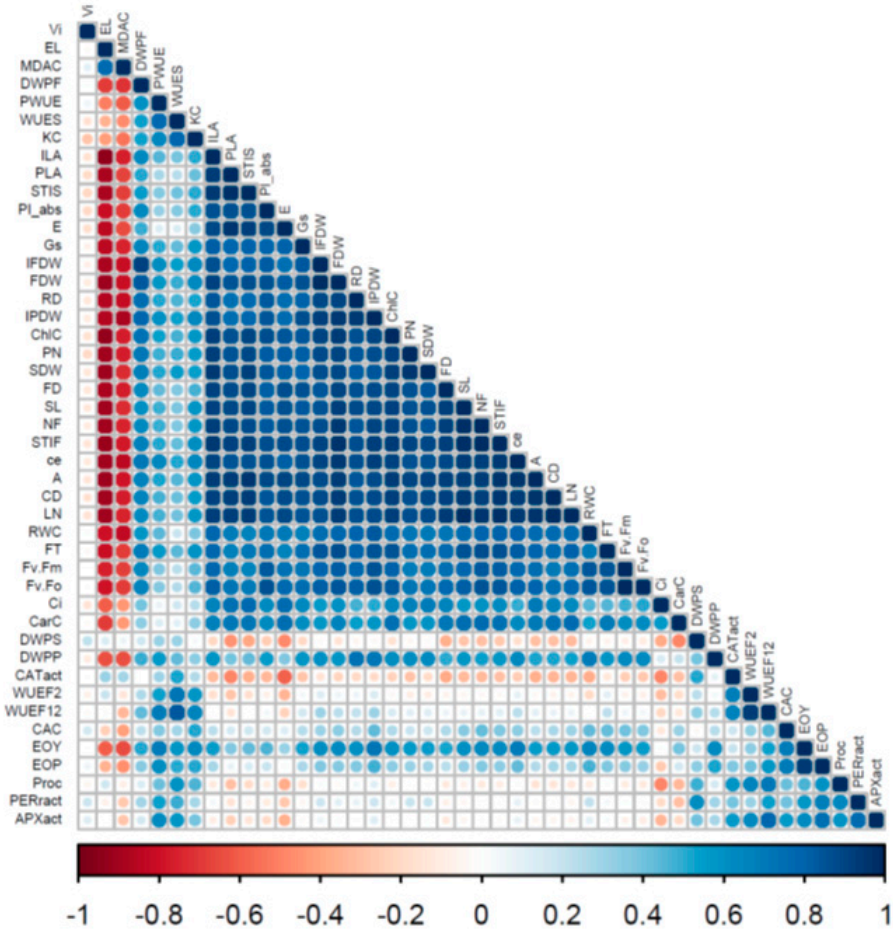

Figure 1. Positive, neutral and negative affinities across morpho-physiological traits in *Rosa damascena* 'Kashan 93' cultivated under different watering regimes (70, 40 and 10% available water content) during two consecutive years. The blue circles represent positive correlations, whereas the red circles convey negative links. Color intensity is correlated by a correlation coefficient (r) on a scale from −1 to 1. Statistically significant values are indicated by larger circles (non-significant, $p = 0.05$, $p = 0.01$ and $p = 0.001$, respectively). A, photosynthesis rate; APXact, ascorbate peroxidase activity; CaC, leaf Ca content; CD, canopy diameter; CarC, carotenoid content; CE, carboxylation efficiency; ChlC, chlorophyll content; C_i, substomatal CO_2 concentration; CATact, catalase activity; DWPF, dry weight (% of total) Flower; DWPP, dry weight (% of total) Petal; DWPS, dry weight (% of total) Shoot; E, transpiration rate; EL, electrolyte leakage; EOP, essential oil; EOY, essential oil yield; FD, flower diameter; FDW, flower dry weight; FN, number of flowers; FT, time to flowering; F_v/F_m, ratio of variable to maximum chlorophyll fluorescence; F_v/F_0, ratio of photochemical to non-photochemical use of light energy in the reaction center of photosystem II; g_s, stomatal conductance; IFDW, individual flower dry weight; ILA, individual leaf area; IPDW, individual petal dry weight; KC, leaf K content; LN, number of leaves; MDAC, MDA content; PI_{abs}, performance index on absorption basis; PLA, plant leaf area; PODact, peroxidase activity; PN, number of petals; ProC, proline content; PWUE, photosynthetic water use efficiency; RD, receptacle diameter; RWC, relative water content; SDW, shoot dry weight; SL, main stem length; STIF, stress tolerance index Flower; STIS, stress tolerance index Shoot; V_j, the relative variable fluorescence at 2 ms; WUEF12, water use efficiency Flower 1 + 2; WUEF2, water use efficiency Flower 2; WUES, water use efficiency Shoot.

3.2. Leaf Chlorophyll Fluorescence

The range of the dark-adapted variable to the maximum fluorescence ratio [$F_v/F_m = (F_m - F_o)/F_m$] was 0.82–0.86, of the ratio of photochemical to non-photochemical use of light energy in the reaction center of photosystem II [$F_v/F_0 = (F_m - F_o)/F_o$] was 4.6–6.0, and of V_j was 0.35–0.48 (Table 1). The performance index on absorption basis (PI_{abs}), which is more sensitive to changes of photosynthetic activity than F_v/F_m, varied between 4.0 and 11.7.

Table 1. Chlorophyll fluorescence features of *Rosa damascena* 'Kashan 93' cultivated under different watering regimes (70, 40 and 10% available water content) during two consecutive years. Values are the mean of three replications ± standard error. F_v/F_0, ratio of photochemical to non-photochemical use of light energy in the reaction center of photosystem II; F_v/F_m, dark-adapted variable to maximum fluorescence ratio; PI_{abs}, performance index on absorption basis; V_j, the relative variable fluorescence at 2 ms.

Year	**1**	**2**	**2**	**2**	**2**	**2**
	Available Water Content (%)		**F_v/F_m**	**F_v/F_0**	**V_j**	**PI_{abs}**
	70	70	0.86 ± 0.001	6.0 ± 0.04	0.35 ± 0.00	11.7 ± 0.01
	70	40	0.84 ± 0.004	5.4 ± 0.04	0.42 ± 0.01	6.50 ± 0.45
	70	10	0.83 ± 0.002	5.1 ± 0.07	0.44 ± 0.01	5.20 ± 0.30
	40	70	0.85 ± 0.002	5.9 ± 0.09	0.39 ± 0.01	9.20 ± 0.49
	40	40	0.85 ± 0.002	5.6 ± 0.10	0.40 ± 0.01	8.20 ± 0.23
	40	10	0.84 ± 0.002	5.6 ± 0.08	0.41 ± 0.01	7.30 ± 0.49
	10	70	0.84 ± 0.002	5.5 ± 0.08	0.42 ± 0.01	6.70 ± 0.37
	10	40	0.83 ± 0.002	4.9 ± 0.07	0.48 ± 0.01	4.00 ± 0.41
	10	10	0.82 ± 0.004	4.6 ± 0.04	0.41 ± 0.03	4.70 ± 0.08
	F-Value		5.28	7.45	5.94	15.31
	p-Value		0.007	<0.001	0.004	<0.001

Across the experimental years (2017−2019), the water deficit (i.e., lower soil available water content) tended to increase V_j, while it tended to decrease F_v/F_m, its interrelated one (F_v/F_0), and PI_{abs} (Table 1), indicating that photo-damage had been induced. This effect was generally more prominent when water deficit was applied in experimental year 2, as compared to experimental year 1. In this way, the largest negative adjustment was achieved during the first year of exposure to water deficit, as compared to the second one.

When pooling all nine treatments [three water deficit regimes (year 1) × three water deficit regimes (year 2)], F_v/F_m was positively correlated with F_v/F_0 and PI_{abs} (R^2 of 0.92 and 0.89, respectively; see also Figure 1).

3.3. Leaf Gas Exchange

Gas exchange traits [photosynthesis rate (3.1–11.8), transpiration rate (1.8–5.3), stomatal conductance (0.30–0.51), substomatal CO_2 concentration (389–585), carboxylation efficiency (0.007–0.022), and photosynthetic water use efficiency (1.7–3.0)] varied by at least 27% among treatments under study (Table 2).

Table 2. Gas exchange features of *Rosa damascena* 'Kashan 93' cultivated under different watering regimes (70, 40 and 10% available water content) during two consecutive years. Values are the mean of three replications ± standard error. PWUE, Photosynthetic water use efficiency.

Year	1	2	2	2	2	2	2	2
	Available Water Content (%)		Photosynthesis Rate (μmol CO_2 m^{-2} s^{-1})	Transpiration Rate (mmol H_2O m^{-2} s^{-1})	Stomatal Conductance (mol m^{-2} s^{-1})	Substomatal CO_2 Concentration (mmol mol^{-1})	Carboxylation Efficiency (mol CO_2 m^{-2} s^{-1})	PWUE (μmol CO_2 mol H_2O^{-1})
	70	70	11.8 ± 0.71	5.3 ± 0.08	0.51 ± 0.043	535 ± 12	0.022 ± 0.0009	2.2 ± 0.11
	70	40	6.10 ± 0.37	2.8 ± 0.24	0.40 ± 0.023	423 ± 26	0.015 ± 0.0011	2.2 ± 0.06
	70	10	3.50 ± 0.20	2.0 ± 0.07	0.33 ± 0.006	432 ± 15	0.008 ± 0.0007	1.8 ± 0.05
	40	70	7.80 ± 0.07	3.8 ± 0.10	0.44 ± 0.028	487 ± 4.3	0.016 ± 0.0001	2.0 ± 0.07
	40	40	8.40 ± 0.41	2.8 ± 0.21	0.44 ± 0.020	464 ± 16	0.018 ± 0.0012	3.0 ± 0.10
	40	10	5.90 ± 0.42	2.4 ± 0.03	0.41 ± 0.006	389 ± 10	0.015 ± 0.0014	2.5 ± 0.20
	10	70	4.90 ± 0.52	2.8 ± 0.17	0.35 ± 0.028	423 ± 34	0.012 ± 0.0003	1.7 ± 0.09
	10	40	4.60 ± 0.04	2.2 ± 0.03	0.33 ± 0.005	426 ± 4.4	0.011 ± 0.0000	2.1 ± 0.04
	10	10	3.10 ± 0.17	1.8 ± 0.18	0.30 ± 0.006	431 ± 14	0.007 ± 0.0004	1.7 ± 0.18
	F-Value		55.89	30.93	4.42	5.76	22.25	5.74
	p-Value		<0.001	<0.001	0.013	0.005	<0.001	0.005

Across experimental years, the water deficit tended to decrease all gas exchange traits (photosynthesis rate, transpiration rate, stomatal conductance, substomatal CO_2 concentration, and carboxylation efficiency), besides photosynthetic water use efficiency where no consistent trend was apparent (Table 2). This negative effect of water deficit on gas exchange traits was generally more prominent when water deficit was applied in experimental year 2, as compared to experimental year 1.

By considering all nine treatments, the photosynthesis rate was positively correlated with the transpiration rate, stomatal conductance, substomatal CO_2 concentration, and carboxylation efficiency (R^2 of 0.86, 0.94, 0.66 and 0.95, respectively; see also Figure 1). These results suggest that plants under water deficit conditions experience limitations in both stomatal and photosynthetic capacity components.

3.4. Plant Phenology, Morphology, Biomass Allocation and Essential Oil Yield

Among treatments, the variation was more prominent in the number of flowers (208–254), individual flower dry weight (0.40–0.52), number of petals (29.3–40.3), receptacle diameter (10.0–12.1), and individual petal dry weight (0.32–0.40), as compared to the time to flowering (79.3–86.7) and flower diameter (65.6–73.5) (Table 3).

Across experimental years, water deficit tended to decrease all floral features under study (time to flowering, number of flowers, flower diameter, individual flower dry weight, number of petals, receptacle diameter, and individual petal dry weight) (Table 3). This negative effect was generally more prominent when water deficit was applied in experimental year 2, as compared to experimental year 1. These results suggest that water deficit conditions simultaneously constrained resource allocation to either aspect of floral display (i.e., size and number).

By pooling all nine treatments, the number of flowers was positively correlated with flower diameter, individual flower dry weight, number of petals, receptacle diameter, and individual petal dry weight (R^2 of 0.95, 0.85, 0.80, 0.85 and 0.88, respectively; see also Figure 1). Therefore, a flower size–number trade-off was clearly not evident across water deficit environments and experimental years.

Table 3. Flowering features of *Rosa damascena* 'Kashan 93' cultivated under different watering regimes (70, 40 and 10% available water content) during two consecutive years. Values are the mean of three replications ± standard error.

Year	1	2	2	2	2	2	2	2	2
	Available Water Content (%)		Time to Flowering (d)	Number of Flowers	Flower Diameter (mm)	Individual Flower Dry Weight (g)	Number of Petals	Receptacle Diameter (mm)	Individual Petal Dry Weight (g)
	70	70	86.7 ± 0.7	254 ± 2	73.5 ± 0.0	0.52 ± 0.004	40.3 ± 0.3	12.1 ± 0.1	0.40 ± 0.003
	70	40	84.3 ± 0.7	232 ± 1	68.8 ± 0.3	0.47 ± 0.009	33.3 ± 0.9	11.4 ± 0.1	0.37 ± 0.003
	70	10	82.3 ± 0.9	221 ± 1	66.4 ± 0.2	0.41 ± 0.002	30.3 ± 0.3	10.1 ± 0.1	0.33 ± 0.003
	40	70	85.3 ± 0.9	238 ± 1	70.4 ± 0.5	0.51 ± 0.023	39.0 ± 0.0	11.8 ± 0.1	0.39 ± 0.002
	40	40	86.3 ± 0.3	238 ± 1	69.9 ± 0.3	0.50 ± 0.017	38.7 ± 0.3	11.6 ± 0.3	0.39 ± 0.008
	40	10	85.0 ± 0.6	234 ± 1	68.8 ± 0.4	0.47 ± 0.005	33.0 ± 0.0	11.4 ± 0.3	0.38 ± 0.006
	10	70	83.7 ± 0.3	228 ± 1	67.8 ± 0.6	0.43 ± 0.010	32.0 ± 1.2	10.7 ± 0.2	0.35 ± 0.007
	10	40	81.0 ± 0.6	226 ± 1	67.4 ± 1.3	0.43 ± 0.004	32.3 ± 0.3	10.4 ± 0.3	0.35 ± 0.009
	10	10	79.3 ± 0.7	208 ± 0	65.6 ± 0.2	0.40 ± 0.003	29.3 ± 1.3	10.0 ± 0.1	0.32 ± 0.006
	F-Value		4.65	115.51	11.10	6.98	11.32	5.57	19.05
	p-Value		0.011	<0.001	<0.001	0.002	<0.001	0.005	<0.001

All traits related to biomass [main stem length (1.50–1.89), canopy diameter (1.51–1.82), number of leaves (594–1301), plant leaf area (0.36–2.09), individual leaf area (5.8–16.1), shoot dry weight (1.46–2.90), flower dry weight (year 1; 0.08–0.13), flower dry weight (year 1 + 2; 0.12–0.20), and shoot dry weight ratio (34.3–45.9)] varied between 17 and 83% among treatments under study (Table 4). The respective variation was 7.9 and 10.7% for the petal dry weight ratio (17.5–19.0) and flower dry weight ratio (16.7–18.7).

Table 4. Morphological, growth and dry weight distribution features of *Rosa damascena* 'Kashan 93' cultivated under different watering regimes (70, 40 and 10% available water content) during two consecutive years. Values are the mean of three replications ± standard error.

Year	1	2	2	2	2	2	2	2	2	2	2
	Available Water Content (%)		Main Stem Length (m)	Canopy Diameter (m^2)	Number of Leaves	Plant Leaf Area (m^2)	Individual Leaf Area (cm^2)	Shoot Dry Weight (kg)	Dry Weight Ratio (%) [1]		
									Shoot	Flower	Petal
	70	70	1.89 ± 0.03	1.82 ± 0.04	1301 ± 46	2.09 ± 0.08	16.1 ± 0.9	2.90 ± 0.11	34.3 ± 0.4	18.1 ± 0.0	18.3 ± 0.13
	70	40	1.68 ± 0.01	1.62 ± 0.00	801 ± 53	0.74 ± 0.05	9.30 ± 0.1	1.71 ± 0.03	41.1 ± 0.6	18.0 ± 0.3	18.3 ± 0.03
	70	10	1.58 ± 0.01	1.51 ± 0.01	594 ± 41	0.40 ± 0.02	6.70 ± 0.2	1.50 ± 0.03	42.0 ± 0.7	16.7 ± 0.1	17.6 ± 0.03
	40	70	1.75 ± 0.00	1.69 ± 0.02	983 ± 58	1.29 ± 0.04	13.2 ± 0.4	2.71 ± 0.02	44.8 ± 0.3	18.7 ± 0.2	19.0 ± 0.05
	40	40	1.73 ± 0.01	1.68 ± 0.02	782 ± 18	0.99 ± 0.02	12.7 ± 0.3	2.67 ± 0.06	45.9 ± 0.5	18.7 ± 0.1	18.9 ± 0.03
	40	10	1.70 ± 0.02	1.63 ± 0.01	706 ± 37	0.65 ± 0.03	9.20 ± 0.6	1.85 ± 0.03	42.1 ± 0.3	18.1 ± 0.2	18.6 ± 0.05
	10	70	1.64 ± 0.02	1.58 ± 0.01	803 ± 64	0.74 ± 0.08	9.20 ± 0.4	1.69 ± 0.03	40.9 ± 0.4	17.0 ± 0.3	18.2 ± 0.01
	10	40	1.62 ± 0.03	1.57 ± 0.03	841 ± 43	0.63 ± 0.04	8.10 ± 0.1	1.69 ± 0.06	41.2 ± 1.1	17.1 ± 0.2	17.9 ± 0.09
	10	10	1.50 ± 0.01	1.51 ± 0.00	615 ± 12	0.36 ± 0.01	5.80 ± 0.2	1.46 ± 0.02	41.1 ± 0.7	16.9 ± 0.1	17.5 ± 0.03
	F-Value		19.38	19.76	13.45	105.15	19.46	61.36	21.80	3.75	4.67
	p-Value		<0.001	<0.001	<0.001	<0.001	<0.001	<0.001	<0.001	0.025	0.011

[1] Dry weight ratio = [(dry weight/fresh weight) × 100].

Across experimental years, water deficit tended to increase shoot dry weight ratio, and decrease the remaining parameters (main stem length, canopy diameter, number of leaves, plant leaf area, individual leaf area, shoot dry weight, flower dry weight, petal dry weight ratio, and flower dry weight ratio) (Table 4, Figure 2). These effects were generally more prominent when water deficit was applied in experimental year 2, as compared to experimental year 1. These results suggest that water deficit conditions not only limited growth, but also elicited specific morphological adjustments.

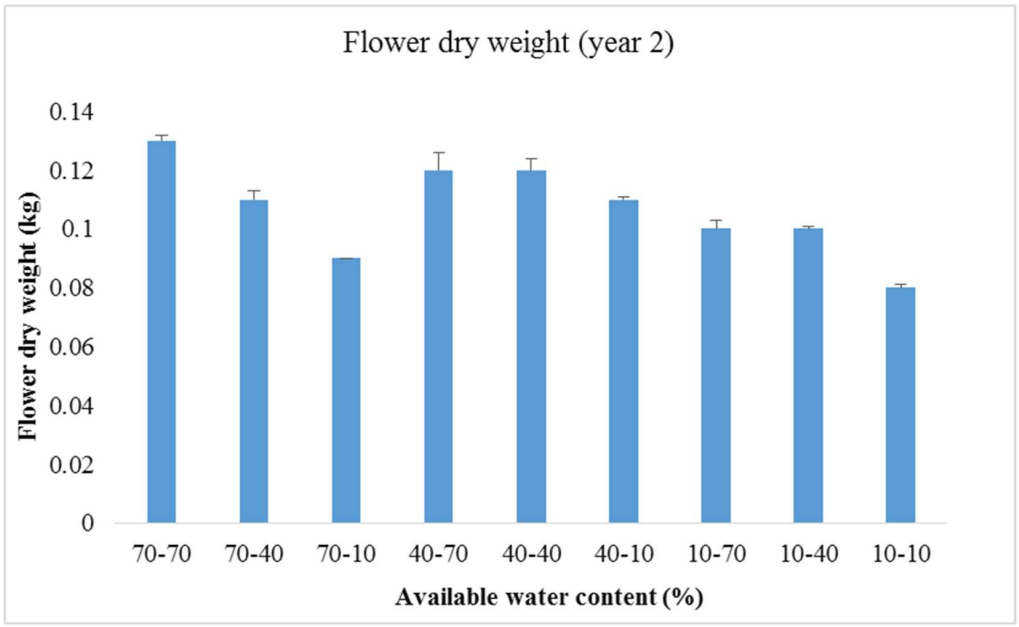

(**A**)

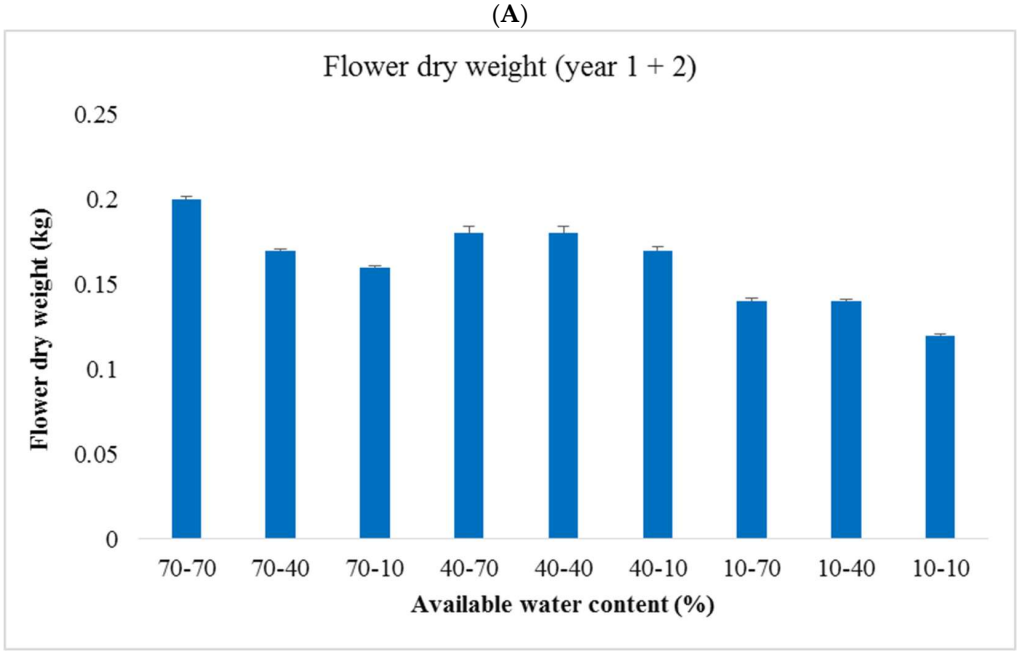

(**B**)

Figure 2. Flower dry weight of year 2 as well as year 1 plus 2 ((**A**,**B**), respectively) in *Rosa damascena* 'Kashan 93' cultivated under different watering regimes (70, 40 and 10% available water content) during two consecutive years. In the x-axis, the former number is the watering regime of year 1, and the latter is the respective one of year 2. Values are the mean of three replications ± the standard error.

By pooling all nine treatments, the number of leaves was positively correlated with plant leaf area, and individual leaf area (R^2 of 0.93, and 0.78, respectively; see also Figure 1). Shoot dry weight was positively related to main stem length (R^2 of 0.78), but was not related to shoot dry weight ratio (R^2 of 0.00; see also Figure 1).

Water use efficiency of the shoot was several orders of magnitude higher than the floral one (Table 5). Water use efficiency [shoot (3.2–6.7), flower (year 2; 0.17–0.35), and flower (year 1 + 2; 0.18–0.28)] varied between 36 and 52% among treatments under study.

Table 5. Water use efficiency (shoot, flower), stress tolerance index (shoot, flower), leaf calcium (Ca) and potassium (K) content as well as petal essential oil percentage and plant essential oil yield of *Rosa damascena* 'Kashan 93' cultivated under different watering regimes (70, 40 and 10% available water content) during two consecutive years. Values are the mean of three replications ± standard error.

Year	1	2	2	2	1 + 2	2	2	2		2	1 + 2
	Available Water Content (%)		Water Use Efficiency (g Dry Mass L^{-1} H_2O)			Stress Tolerance Index (%)		Leaf Ca Content	Leaf K Content	Essential Oil (%)	Essential Oil Yield (g $plant^{-1}$)
			Shoot	Flower	Flower	Shoot	Flower	($\mu g\ g^{-1}$)			
	70	70	5.2 ± 0.1	0.23 ± 0.003	0.21 ± 0.000	100 ± 2.6	100 ± 1.5	252 ± 8.30	228 ± 2.50	0.027 ± 0.001	0.19 ± 0.01
	70	40	4.3 ± 0.1	0.27 ± 0.006	0.22 ± 0.003	49.3 ± 0.4	82.9 ± 0.9	217 ± 15.9	196 ± 16.9	0.026 ± 0.003	0.16 ± 0.02
	70	10	4.7 ± 0.1	0.28 ± 0.000	0.22 ± 0.000	42.4 ± 0.7	74.3 ± 0.4	223 ± 8.10	200 ± 2.20	0.022 ± 0.002	0.12 ± 0.01
	40	70	4.8 ± 0.1	0.21 ± 0.009	0.21 ± 0.006	71.9 ± 1.4	89.0 ± 0.9	234 ± 3.20	195 ± 4.90	0.027 ± 0.003	0.17 ± 0.02
	40	40	6.7 ± 0.1	0.3 ± 0.012	0.26 ± 0.006	69.0 ± 0.6	88.7 ± 1.0	253 ± 3.30	234 ± 0.90	0.038 ± 0.001	0.24 ± 0.01
	40	10	5.8 ± 0.1	0.35 ± 0.003	0.28 ± 0.003	52.1 ± 0.9	84.3 ± 0.1	314 ± 21.2	230 ± 4.80	0.040 ± 0.001	0.25 ± 0.01
	10	70	3.2 ± 0.1	0.17 ± 0.003	0.18 ± 0.003	49.2 ± 0.9	79.6 ± 0.6	245 ± 10.7	176 ± 3.00	0.030 ± 0.002	0.17 ± 0.01
	10	40	4.2 ± 0.1	0.24 ± 0.000	0.22 ± 0.000	48.7 ± 0.8	78.1 ± 1.2	275 ± 14.4	192 ± 17.5	0.030 ± 0.000	0.17 ± 0.00
	10	10	4.5 ± 0.1	0.26 ± 0.000	0.22 ± 0.000	42.2 ± 0.9	68.0 ± 0.3	188 ± 10.2	182 ± 6.10	0.021 ± 0.001	0.10 ± 0.01
	F-Value		51.10	26.76	36.86	199.75	82.88	14.02	5.86	10.37	16.17
	p-Value		<0.001	<0.001	<0.001	<0.001	<0.001	<0.001	0.004	<0.001	<0.001

The water deficit effect on shoot water use efficiency did not follow a general trend (Table 5). At 70% available water content of experimental year 2, the water deficit during experimental year 1 tended to decrease floral water use efficiency. Within each water deficit regime of experimental year 1, water deficit during experimental year 2 tended to increase floral water use efficiency.

The stress tolerance index of the flower was higher than the one of the shoot (68–100 versus 42–100; Table 5).

Across experimental years, the water deficit tended to decrease shoot and flower stress tolerance index (Table 5). These effects were generally more prominent on the shoot as compared to the flower, as well as when the water deficit was applied in experimental year 2, as compared to experimental year 1. This finding has the interesting implication that reproductive modules generally appear more tolerant to water deficit conditions, as compared to plant size.

Petal essential oil percentage varied between 0.021 and 0.040, while plant essential oil yield between 0.10 and 0.25 (Table 5).

At 70% available water content of experimental year 1, the water deficit during experimental year 2 tended to decrease petal essential oil percentage and plant essential oil yield (Table 5). At 40% available water content of experimental year 1, water deficit during experimental year 2 tended to increase petal essential oil percentage and plant essential oil yield. At 10% available water content of experimental year 1, water deficit during experimental year 2 decreased petal essential oil percentage and plant essential oil yield only at 10% available water content.

By pooling all nine treatments, a strong correlation was apparent between the petal essential oil percentage and plant essential oil yield (R^2 of 0.91; see also Figure 1).

The water deficit effect on leaf Ca and K contents did not follow a general trend (Table 5).

3.5. Plant Physiological and Biochemical Traits

Across experimental years, the water deficit tended to increase electrolyte leakage (indicating stress-induced tissue injury), decrease leaf relative water content (thus hydration level), as well as chlorophyll and carotenoid (major photosynthetic pigments with the latter also being major non-enzymatic antioxidant) contents (Table 6). These effects were generally more prominent when water deficit was applied in experimental year 2, as compared to experimental year 1.

Table 6. Relative water content, electrolyte leakage, content of chlorophyll, carotenoids, malondialdehyde (MDA), and proline, as well as catalase, peroxidase and ascorbate peroxidase activity of *Rosa damascena* 'Kashan 93' cultivated under different watering regimes (70, 40 and 10% available water content) during two consecutive years. Values are the mean of three replications ± standard error. FW, fresh weight.

Year	1	2	2	2	2	2	2	2	2	2	2
	Available Water Content (%)		Relative Water Content (%)	Electrolyte Leakage (%)	Chlorophyll	Carotenoid	MDA	Proline	Catalase	Peroxidase	Ascorbate Peroxidase
					Content (mg g^{-1} FW)		Content (µmol g^{-1} FW)		Activity (µmol min^{-1} g^{-1} FW)		
	70	70	67.7 ± 0.6	19.3 ± 0.1	18.8 ± 0.87	4.0 ± 0.51	0.9 ± 0.03	2.6 ± 0.09	1.4 ± 0.10	0.36 ± 0.016	0.12 ± 0.006
	70	40	62.0 ± 1.6	29.4 ± 0.1	11.8 ± 0.56	2.5 ± 0.25	1.2 ± 0.10	2.8 ± 0.09	1.6 ± 0.11	0.38 ± 0.039	0.14 ± 0.002
	70	10	50.0 ± 0.6	39.4 ± 0.9	8.70 ± 0.15	2.0 ± 0.08	2.1 ± 0.24	3.5 ± 0.12	2.0 ± 0.05	0.41 ± 0.004	0.13 ± 0.003
	40	70	65.8 ± 1.7	22.3 ± 0.2	15.9 ± 0.85	2.7 ± 0.24	1.0 ± 0.05	3.0 ± 0.10	1.6 ± 0.04	0.49 ± 0.009	0.14 ± 0.014
	40	40	65.6 ± 0.5	24.5 ± 1.0	16.1 ± 0.66	2.6 ± 0.17	1.0 ± 0.02	4.2 ± 0.34	2.1 ± 0.07	0.62 ± 0.019	0.23 ± 0.013
	40	10	61.8 ± 1.5	30.0 ± 0.3	12.9 ± 0.85	2.5 ± 0.13	1.0 ± 0.11	4.5 ± 0.27	2.1 ± 0.09	0.52 ± 0.031	0.25 ± 0.008
	10	70	63.5 ± 1.0	30.0 ± 0.4	11.5 ± 0.45	2.8 ± 0.15	1.6 ± 0.18	2.7 ± 0.20	1.5 ± 0.06	0.43 ± 0.009	0.13 ± 0.002
	10	40	61.1 ± 0.6	33.8 ± 0.5	9.30 ± 0.75	2.0 ± 0.10	1.4 ± 0.07	3.4 ± 0.11	1.6 ± 0.04	0.56 ± 0.014	0.21 ± 0.018
	10	10	51.1 ± 4.3	38.0 ± 2.0	8.10 ± 0.31	1.7 ± 0.06	1.7 ± 0.14	3.2 ± 0.09	1.9 ± 0.01	0.43 ± 0.002	0.16 ± 0.001
	F-Value		5.28	21.86	15.90	4.36	12.39	3.37	1.95	6.47	18.33
	p-Value		0.007	<0.001	<0.001	0.014	<0.001	0.035	0.152	0.003	<0.001

With the exception of 40% available water content of experimental year 1, water deficit tended to increase leaf MDA content (Table 6), indicating enhanced levels of lipid peroxidation. Across experimental years, water deficit also tended to increase leaf proline content, which is an excellent osmolyte.

Across experimental years, water deficit also tended to enhance the activity of three key antioxidant enzymes (CAT, POD, and APX; Table 6).

By pooling all nine treatments, leaf relative water content (thus hydration level) was positively correlated with both tissue damage indices (i.e., electrolyte leakage, and leaf MDA content, R^2 of 0.77, and 0.75, respectively; see also Figure 1). A strong correlation was apparent between electrolyte leakage and leaf MDA content (R^2 of 0.76), as well as between leaf chlorophyll and carotenoid contents (R^2 of 0.76; see also Figure 1).

3.6. Principal Component Analysis

To identify and measure the components that control the influence across the treatments, a PCA was performed (Figure 3). The eigenvalues were assessed to ascertain the number of optimal principal components. The first two dimensions supported 76.6% of the total variation (Figures S1 and S2). The degree of a considerable impact of each trait reflected on the PCA was assessed by employing the cos 2 index. Amongst these descriptors, electrolyte leakage, MDA content, chlorophyll content, flower dry weight, the number of leaves and transpiration rate had a great imprint for the classification of individual units. The PCA, established on the first two components, disclosed the complicated association between the treatments (Figure 3).

Interestingly, water availability across the years was not a factor that enabled a clear cut-off value for damask rose traits. Specifically, phenotypes that had a watering scheme of 40% available water content during the first year were indistinguishable during the second year, when irrigated at 40 or 10% available water content. On the other hand, 10% available water content during the second year was vital for the grouping of units that were first irrigated at 70 and 10% available water content thresholds. Nonetheless, well-watered roses across both years (constant 70% available water content) formed a separate cluster, signifying that irrigation is a crucial parameter for developing specific agronomical and biochemical traits.

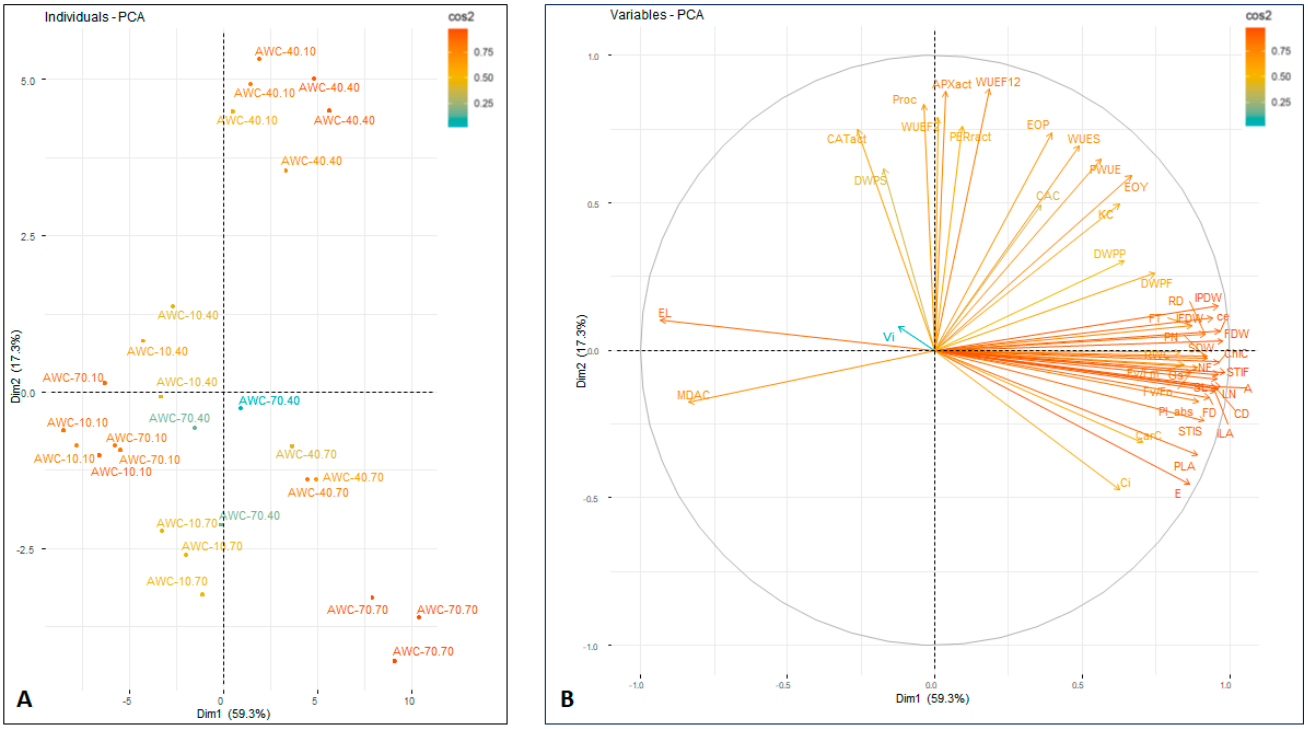

Figure 3. (**A**) Principal coordinate analysis across *Rosa damascena* 'Kashan 93' cultivated under different watering regimes (70, 40 and 10% available water content) during two consecutive years. (**B**) A gradient scale and color intensity (scale) show how each attribute contributes to the two dimensions. Lower cos2 values are found in vectors close to the plot center. Variables with narrow angles show affinity, whereas those with broad angles show a negative connection. A, photosynthesis rate; APXact, ascorbate peroxidase activity; CaC, leaf Ca content; CD, canopy diameter; CarC, carotenoid content; CE, carboxylation efficiency; ChlC, chlorophyll content; C_i, substomatal CO_2 concentration; CATact, catalase activity; DWPF, dry weight (% of total) Flower; DWPP, dry weight (% of total) Petal; DWPS, dry weight (% of total) Shoot; E, transpiration rate; EL, electrolyte leakage; EOP, essential oil; EOY, essential oil yield; FD, flower diameter; FDW, flower dry weight; FN, number of flowers; FT, time to flowering; F_v/F_m, ratio of variable to maximum chlorophyll fluorescence; F_v/F_0, ratio of photochemical to non-photochemical use of light energy in the reaction center of photosystem II; g_s, stomatal conductance; IFDW, individual flower dry weight; ILA, individual leaf area; IPDW, individual petal dry weight; KC, leaf K content; LN, number of leaves; MDAC, MDA content; PI_{abs}, performance index on absorption basis; PLA, plant leaf area; PODact, peroxidase activity; PN, number of petals; ProC, proline content; PWUE, photosynthetic water use efficiency; RD, receptacle diameter; RWC, relative water content; SDW, shoot dry weight; SL, main stem length; STIF, stress tolerance index Flower; STIS, stress tolerance index Shoot; V_j, the relative variable fluorescence at 2 ms; WUEF12, water use efficiency Flower 1 + 2; WUEF2, water use efficiency Flower 2; WUES, water use efficiency Shoot.

4. Discussion

In environments with low or unpredictable precipitation, soil water deficit inevitably poses serious challenges to plant growth and productivity [12,13]. By using different soil water deficit levels spanning over two growing seasons in a field experiment carried out in a semi-arid region, the long-term acclimation responses of damask rose to water limitation were assessed for the first time, along with the underlying morphological, physiological and biochemical processes.

Soil water shortage limited plant growth and essential oil yield (Tables 4 and 5). This effect was amplified, as soil water deficit became more intense. Previous studies have also indicated that water limitation effects on plant growth and productivity are incremental as water availability decreases [9,15]. Notably, this inhibition of plant growth and essential

oil yield was less pronounced, when plants had been exposed to water severity during the preceding year (Tables 4 and 5). In a single growth season, where water deficit had been imposed over weeks, evidence of water stress memory has been earlier documented in other taxa (e.g., *Alopecurus pratensis* [37], *Solanum tuberosum* [38]). Under water deficit over seasons, instead, water stress memory effects have been reported in a limited number of species (e.g., *Vitis vinifera*; [12]). Our findings in the present study directly suggest that exposure to water deficit elicits plant tolerance to future exposure in next seasons. In this regard, this study for the first time provides evidence for stress memory in damask rose. This phenotypic response was further dependent on the water deficit level (Tables 4 and 5). At more intense soil water deficit across the preceding year, plants were less vulnerable to water deficit during the subsequent one. Therefore, our results reveal a link between water deficit severity and plant tolerance to future water stress challenges.

Reduced soil water availability markedly affected all aspects of plant growth and development under study. For instance, it was related to quicker completion of the growth cycle, as illustrated by earlier flowering (up to 7.4 d), to lower number of flowers and to decreased floral size (Table 3). In terms of time to flowering, an early transition from vegetative to reproductive phase reduces the period available for carbon fixation during the vegetative stage, and in this way is conventionally counterproductive in terms of yield [9,15]. In other species, acceleration of floral transition has been associated with decreased duration of leaf expansion [39]. Reduced soil water availability was further associated with smaller plants (Table 4). Although the decrease in size was indeed expressed across all organs under study (i.e., stem, leaves, and flowers), it was not uniform (Tables 3 and 4, Figure 2). In this way, water deficit elicited a range of morphological adaptations, including biomass partitioning adjustments (Table 4, Figure 2).

The water deficit-induced decrease in plant size was mediated by several morphological and physiological traits. Under such conditions, biomass accumulation was incrementally constrained by lower leaf area (Table 4), chlorophyll content (Table 6), CO_2 intake (Table 2), and photosynthetic efficiency (Tables 1 and 2). Comparable findings have been earlier noted in other taxa [9,14,16]. The decrease in CO_2 intake was driven by a reduction in stomatal conductance (Table 2), since under such conditions stomata tend to close under the need to conserve hydration [12,40]. The decrease in plant leaf area (up to 83%) was mediated by reductions in both number of leaves (up to 54%), and individual leaf area (up to 64%). Contrary to our findings, in another study on damask rose, where water stress was realized in a single season, leaf number was not affected by water limitation [8].

Water deficit has been earlier related to increased water use efficiency [41]. In this study and against expectations, photosynthetic water use efficiency (Table 2), and water use efficiency of the shoot (Table 5) were not consistently affected by soil water deficit. At 70% available water content imposed during experimental year 2, water deficit during experimental year 1 tended to decrease floral water use efficiency (Table 5). Within each water deficit regime of experimental year 1, water deficit during experimental year 2 tended to increase floral water use efficiency. In our study system, therefore, soil water deficit determined floral water use efficiency, and this effect was dependent on the timing (year) of water severity.

A strong positive correlation between petal essential oil percentage and plant essential oil yield was evident (R^2 of 0.91; see also Figure 1). These two traits co-varied based on both water deficit level and year of exposure. At 70 and 10% available water content of experimental year 1, water deficit during experimental year 2 tended to decrease petal essential oil percentage and plant essential oil yield (Table 5). At 40% available water content of experimental year 1, instead, water deficit during experimental year 2 tended to increase petal essential oil percentage and plant essential oil yield. In this way, petal essential oil percentage and plant essential oil yield always varied in the same direction in response to soil water deficit, while the sign of this response (positive or negative) was dependent on the timing (year) of water severity.

Water deficit elicits oxidative stress [14]. In this study, it was indeed related to enhanced electrolyte leakage (Table 6), indicating impaired membrane integrity [15,16]. At water deficit conditions, membrane damage is typically a symptom of oxidative damage, arising when ROS accumulation reaches phytotoxic levels [9,15]. The scavenging system was further assessed by determining proline and carotenoid contents, as well as CAT, POD, and APX activities (Table 6). Under water deficit conditions, carotenoid content was generally downregulated. Instead, proline synthesis and the activity of the three antioxidant enzymes were rather stimulated (Table 6), which jointly are expected to narrow the oxidative burst and the associated cell damage.

5. Conclusions

Across two experimental years, the quantitative relationship between water deficit severity and plant phenotype was investigated. Plants were subjected to three different water deficit levels for two periods (June–October). Water deficit shortened the time required for the transition from the vegetative to reproductive phase (up to 7.4 d), and constrained resource allocation to either aspect of floral display (size and number). Across treatments, a trade-off between flower size and number was clearly not apparent. Soil water deficit was also related to smaller plants (up to 49.7%). Despite the noted activation of the ROS scavenging system, oxidative stress symptoms were still elicited by water deficit. Plant hydration level was closely associated with two tissue injury indices. These effects were generally amplified, as soil water deficit became more severe. Importantly, the adverse effects of water deficit were mostly less pronounced, when plants had been exposed to water deficit during the preceding year. Therefore, exposure to water deficit enhanced plant tolerance to future exposure. This phenotypic response was further dependent on the water deficit level. At a more severe soil water deficit across the preceding year, plants were less vulnerable to water deficit during the subsequent one. Therefore, our results suggest a consistent relationship between water deficit severity and plant tolerance to future water stress challenges, providing for the first time evidence for stress memory existence in damask rose.

Supplementary Materials: The following supporting information can be downloaded at: https://www.mdpi.com/article/10.3390/horticulturae10050462/s1, Figure S1: The experimental layout (A), and field (B), where this study was conducted. Each plot contained four lines of 10 plants. At each plot, measurements were performed on three randomly selected plants situated at lines 2 and 3. In each plant, three separate measurements were obtained. The average of these nine measurements per plot was further treated as a single replication. For taking observations, three plots were analyzed. Figure S2: Ten major components along with the proportions of ascribed variance. The principal component analysis biplot (which accounts for 76.6% of the cumulative percentage explained) was created using the first two eigenvalues.

Author Contributions: Conceptualization, A.R.N. and D.F.; methodology, F.A., A.R.N., S.M.-F., M.R. and D.F.; software, N.N. and D.F.; validation, E.G. and D.F.; formal analysis, N.N., E.G. and D.F.; resources, A.R.N. and S.M.-F.; data curation, F.A., A.R.N., S.M.-F., N.N. and D.F.; writing—original draft preparation, F.A. and D.F.; writing—review and editing, N.N., A.R.N., E.G. and D.F.; supervision, A.R.N. and D.F.; project administration and funding acquisition, A.R.N. and S.M.-F. All authors have read and agreed to the published version of the manuscript.

Funding: This research was financed by Lorestan University (Iran).

Data Availability Statement: Raw data are available upon request from the corresponding author.

Acknowledgments: The authors gratefully acknowledge the laboratory crew for their inputs, continued attentiveness and lifelong dedication to service. The valuable comments of the editor and three anonymous reviewers are greatly appreciated.

Conflicts of Interest: The authors declare no conflicts of interest.

Abbreviations

APX, ascorbate peroxidase; CAT, catalase; FW, fresh weight; F_v/F_m, ratio of variable to maximum chlorophyll fluorescence; F_v/F_0, ratio of photochemical to non-photochemical use of light energy in the reaction center of photosystem II; MDA, malondialdehyde; PCA, principal component analysis; PI_{abs}, performance index on absorption basis; POD, peroxidase; PWUE, photosynthetic water use efficiency; ROS, reactive oxygen species; RWC, relative water content; V_j, the relative variable fluorescence at 2 ms.

References

1. Kovacheva, N.; Rusanov, K.; Atanassov, I. Industrial cultivation of oil bearing rose and rose oil production in Bulgaria during 21st century, directions and challenges. *Biotechnol. Biotechnol. Equip.* **2010**, *24*, 1793–1798. [CrossRef]
2. Kumar, A.; Gautam, R.D.; Singh, S.; Chauhan, R.; Kumar, M.; Kumar, D.; Kumar, A.; Singh, S. Phenotyping floral traits and essential oil profiling revealed considerable variations in clonal selections of damask rose (*Rosa damascena* Mill.). *Sci. Rep.* **2023**, *13*, 8101. [CrossRef] [PubMed]
3. Omidi, M.; Khandan-Mirkohi, A.; Kafi, M.; Rasouli, O.; Shaghaghi, A.; Kiani, M.; Zamani, Z. Comparative study of phytochemical profiles and morphological properties of some Damask roses from Iran. *Chem. Biol. Technol. Agric.* **2022**, *9*, 51. [CrossRef]
4. Yaghoobi, M.; Farimani, M.M.; Sadeghi, Z.; Asghari, S.; Rezadoost, H. Chemical analysis of Iranian *Rosa damascena* essential oil, concrete, and absolute oil under different bio-climatic conditions. *Ind. Crops Prod.* **2022**, *187*, 115266. [CrossRef]
5. Venkatesha, K.T.; Gupta, A.; Rai, A.N.; Jambhulkar, S.J.; Bisht, R.; Padalia, R.C. Recent developments, challenges, and opportunities in genetic improvement of essential oil-bearing rose (*Rosa damascena*): A review. *Ind. Crops Prod.* **2022**, *184*, 114984. [CrossRef]
6. Kumar, R.; Sharma, S.; Sood, S.; Agnihotri, V.K.; Singh, V.; Singh, B. Evaluation of several *Rosa damascena* varieties and *Rosa bourboniana* accession for essential oil content and composition in western Himalayas. *J. Essent. Oil Res.* **2014**, *26*, 147–152. [CrossRef]
7. Nunes, H.; Miguel, M.G. *Rosa damascena* essential oils: A brief review about chemical composition and biological properties. *Trends Phytochem. Res.* **2017**, *1*, 111–128.
8. Al-Yasi, H.; Attia, H.; Alamer, K.; Hassan, F.; Ali, E.; Elshazly, S.; Siddique, K.H.; Hessini, K. Impact of drought on growth, photosynthesis, osmotic adjustment, and cell wall elasticity in Damask rose. *Plant Physiol. Biochem.* **2020**, *150*, 133–139. [CrossRef]
9. Yang, X.; Lu, M.; Wang, Y.; Wang, Y.; Liu, Z.; Chen, S. Response mechanism of plants to drought stress. *Horticulturae* **2021**, *7*, 50. [CrossRef]
10. Seifikalhor, M.; Niknam, V.; Aliniaeifard, S.; Didaran, F.; Tsaniklidis, G.; Fanourakis, D.; Teymoorzadeh, M.; Mousavi, S.H.; Bosacchi, M.; Li, T. The regulatory role of γ-Aminobutyric acid in chickpea plants depends on drought tolerance and water scarcity level. *Sci. Rep.* **2022**, *12*, 7034. [CrossRef]
11. Yousefzadeh, K.; Houshmand, S.; Shiran, B.; Mousavi-Fard, S.; Zeinali, H.; Nikoloudakis, N.; Gheisari, M.M.; Fanourakis, D. Joint effects of developmental stage and water deficit on essential oil traits (content, yield, composition) and related gene expression: A case study in two *Thymus* species. *Agronomy* **2022**, *12*, 1008. [CrossRef]
12. Tombesi, S.; Frioni, T.; Poni, S.; Palliotti, A. Effect of water stress "memory" on plant behavior during subsequent drought stress. *Environ. Exp. Bot.* **2018**, *150*, 106–114. [CrossRef]
13. Seleiman, M.F.; Al-Suhaibani, N.; Ali, N.; Akmal, M.; Alotaibi, M.; Refay, Y.; Dindaroglu, T.; Abdul-Wajid, H.H.; Battaglia, M.L. Drought stress impacts on plants and different approaches to alleviate its adverse effects. *Plants* **2021**, *10*, 259. [CrossRef]
14. Abdallah, M.B.; Methenni, K.; Nouairi, I.; Zarrouk, M.; Youssef, N.B. Drought priming improves subsequent more severe drought in a drought-sensitive cultivar of olive cv. *Chétoui. Sci. Hortic.* **2017**, *221*, 43–52. [CrossRef] [PubMed]
15. Zomorrodi, N.; Rezaei Nejad, A.; Mousavi-Fard, S.; Feizi, H.; Nikoloudakis, N.; Fanourakis, D. Efficiency of sodium and calcium chloride in conferring cross-tolerance to water deficit in periwinkle. *Horticulturae* **2022**, *8*, 1091. [CrossRef]
16. Zomorrodi, N.; Rezaei Nejad, A.; Mousavi-Fard, S.; Feizi, H.; Tsaniklidis, G.; Fanourakis, D. Potency of titanium dioxide nanoparticles, sodium hydrogen sulfide and salicylic acid in ameliorating the depressive effects of water deficit on periwinkle ornamental quality. *Horticulturae* **2022**, *8*, 675. [CrossRef]
17. Sachdev, S.; Ansari, S.A.; Ansari, M.I.; Fujita, M.; Hasanuzzaman, M. Abiotic stress and reactive oxygen species: Generation, signaling, and defense mechanisms. *Antioxidants* **2021**, *10*, 277. [CrossRef] [PubMed]
18. Hassan, F.A.S.; Ali, E.F.; Alamer, K.H. Exogenous application of polyamines alleviates water stress-induced oxidative stress of *Rosa damascena* Miller var. trigintipetala Dieck. *S. Afr. J. Bot.* **2018**, *116*, 96–102. [CrossRef]
19. Kulak, M. Recurrent drought stress effects on essential oil profile of Lamiaceae plants: An approach regarding stress memory. *Ind. Crops Prod.* **2020**, *154*, 112695. [CrossRef]
20. Jacques, C.; Salon, C.; Barnard, R.L.; Vernoud, V.; Prudent, M. Drought stress memory at the plant cycle level: A review. *Plants* **2021**, *10*, 1873. [CrossRef]

21. Lämke, J.; Bäurle, I. Epigenetic and chromatin-based mechanisms in environmental stress adaptation and stress memory in plants. *Genome Biol.* **2017**, *18*, 124. [CrossRef] [PubMed]
22. Li, X.; Liu, F. Drought stress memory and drought stress tolerance in plants: Biochemical and molecular basis. In *Drought Stress Tolerance in Plants, Vol 1: Physiology and Biochemistry*; Springer: Cham, Switzerland, 2016; pp. 17–44.
23. Bruce, T.J.A.; Matthes, M.C.; Napier, J.A.; Pickett, J.A. Stressful "memories" of plants: Evidence and possible mechanisms. *Plant Sci.* **2007**, *173*, 603–608. [CrossRef]
24. Alves, R.D.; Menezes-Silva, P.E.; Sousa, L.F.; Loram-Lourenço, L.; Silva, M.L.; Almeida, S.E.; Silva, F.G.; Perez de Souza, L.; Fernie, A.R.; Farnese, F.S. Evidence of drought memory in *Dipteryx alata* indicates differential acclimation of plants to savanna conditions. *Sci. Rep.* **2020**, *10*, 16455. [CrossRef] [PubMed]
25. Moosavi-Nezhad, M.; Salehi, R.; Aliniaeifard, S.; Tsaniklidis, G.; Woltering, E.J.; Fanourakis, D.; Żuk-Gołaszewska, K.; Kalaji, H.M. Blue light improves photosynthetic performance during healing and acclimatization of grafted watermelon seedlings. *Int. J. Mol. Sci.* **2021**, *22*, 8043. [CrossRef]
26. Barboričová, M.; Filaček, A.; Vysoka, D.M.; Gašparovič, K.; Živčák, M.; Brestič, M. Sensitivity of fast chlorophyll fluorescence parameters to combined heat and drought stress in wheat genotypes. *Plant Soil Environ.* **2022**, *68*, 309–316. [CrossRef]
27. Jańczak-Pieniążek, M.; Pikuła, W.; Pawlak, R.; Drygaś, B.; Szpunar-Krok, E. Physiological response of *Miscanthus sinensis* (Anderss.) to biostimulants. *Agriculture* **2023**, *14*, 33. [CrossRef]
28. Fanourakis, D.; Heuvelink, E.; Carvalho, S.M. Spatial heterogeneity in stomatal features during leaf elongation: An analysis using *Rosa hybrida*. *Funct. Plant Biol.* **2015**, *42*, 737–745. [CrossRef] [PubMed]
29. Jia, X.; Lyu, Y. Comparative transcriptome and weighted gene co-expression network analysis identify key transcription factors of *Rosa chinensis* 'Old Blush' after exposure to a gradual drought stress followed by recovery. *Front. Genet.* **2021**, *12*, 690264. [CrossRef]
30. Gohari, G.; Mohammadi, A.; Akbari, A.; Panahirad, S.; Dadpour, M.R.; Fotopoulos, V.; Kimura, S. Titanium dioxide nanoparticles (TiO_2 NPs) promote growth and ameliorate salinity stress effects on essential oil profile and biochemical attributes of *Dracocephalum moldavica*. *Sci. Rep.* **2020**, *10*, 912. [CrossRef]
31. Zakerian, F.; Sefidkon, F.; Abbaszadeh, B.; Kalate Jari, S. Effects of Water stress and mycorrhizal fungi on essential oil content and composition of *Satureja sahendica* Bornm. *J. Agric. Sci. Technol.* **2020**, *22*, 789–799.
32. F Larbi, A.; Kchaou, H.; Gaaliche, B.; Gargouri, K.; Boulal, H.; Morales, F. Supplementary potassium and calcium improves salt tolerance in olive plants. *Sci. Hortic.* **2020**, *260*, 108912. [CrossRef]
33. Lichtenthaler, H.K.; Wellburn, A.R. Determinations of total carotenoids and chlorophylls a and b of leaf extracts in different solvents. *Biochem. Soc. Trans.* **1983**, *11*, 591–592. [CrossRef]
34. Fanourakis, D.; Papadakis, V.M.; Machado, M.; Psyllakis, E.; Nektarios, P.A. Non-invasive leaf hydration status determination through convolutional neural networks based on multispectral images in chrysanthemum. *Plant Growth Regul.* **2024**, *102*, 485–496. [CrossRef]
35. Safaei Far, A.; Mousavi-Fard, S.; Rezaei Nejad, A.; Shahbazi, F.; Ahmadi-Majd, M.; Fanourakis, D. Nano Silver and melatonin effectively delay the senescence of cut carnation flowers under simulated vibrational stress. *J. Hortic. Sci. Biotech.* **2024**. [CrossRef]
36. Ahmadi-Majd, M.; Mousavi-Fard, S.; Rezaei Nejad, A.; Fanourakis, D. Nano-selenium in the holding solution promotes rose and carnation vase life by improving both water relations and antioxidant status. *J. Hortic. Sci. Biotech.* **2023**, *98*, 246–261. [CrossRef]
37. Lukić, N.; Kukavica, B.; Davidović-Plavšić, B.; Hasanagić, D.; Walter, J. Plant stress memory is linked to high levels of anti-oxidative enzymes over several weeks. *Environ. Exp. Bot.* **2020**, *178*, 104166. [CrossRef]
38. Ramírez, D.A.; Rolando, J.L.; Yactayo, W.; Monneveux, P.; Mares, V.; Quiroz, R. Improving potato drought tolerance through the induction of long-term water stress memory. *Plant Sci.* **2015**, *238*, 26–32. [CrossRef]
39. Schmalenbach, I.; Zhang, L.; Reymond, M.; Jiménez-Gómez, J.M. The relationship between flowering time and growth responses to drought in the *Arabidopsis* Landsberg erecta x Antwerp-1 population. *Front. Plant Sci.* **2014**, *5*, 107219. [CrossRef] [PubMed]
40. Meinzer, F.C. Stomatal control of transpiration. *Trends Ecol. Evol.* **1993**, *8*, 289–294. [CrossRef]
41. Kapoor, D.; Bhardwaj, S.; Landi, M.; Sharma, A.; Ramakrishnan, M.; Sharma, A. The impact of drought in plant metabolism: How to exploit tolerance mechanisms to increase crop production. *Appl. Sci.* **2020**, *10*, 5692. [CrossRef]